Available at www.sciencedirect.com

ScienceDirect

journal homepage: www.elsevier.com/locate/he

Liquid phase-enabled reaction of Al–Ga and Al–Ga–In–Sn alloys with water

Jeffrey T. Ziebarth [a,*], Jerry M. Woodall [a,**], Robert A. Kramer [b], Go Choi [a]

[a] Purdue University, 465 Northwestern Ave, West Lafayette, IN 47907, United States
[b] Purdue University, 2200 169th Street, Hammond, IN 46323, United States

ARTICLE INFO

Article history:
Received 14 September 2010
Received in revised form
18 January 2011
Accepted 22 January 2011
Available online 24 February 2011

Keywords:
Hydrogen
Aluminum
Water splitting
Liquid phase
Reaction mechanism

ABSTRACT

The water-reactivity of Al–Ga and Al–Ga–In–Sn alloys is investigated as a means to utilize the chemical potential energy of Al to split water for the production of H_2. Al in bulk quantities of these alloys participates in a heterogeneous reaction with water to produce H_2 and α-$Al(OH)_3$ (bayerite). Low melting point phases in these alloys are believed to enable the observed reaction upon liquefaction by providing a means of transport for Al in the alloys to reach a reaction site. In the Al–Ga binary system, this reaction-enabling phase is shown to form at a temperature corresponding to the system's eutectic melting point. In the Al–Ga–In–Sn quaternary system this reaction-enabling phase liquefies at 9.38 °C, as shown using differential scanning calorimetry (DSC). Alloys with the composition 50 wt% Al-34 wt% Ga-11 wt% In-5 wt% Sn are reacted with distilled water in a series of controlled experiments, and H_2 yield from these reactions is measured as a function of time and temperature. Applying kinetic analysis to the yield data shows the apparent activation energy for the reaction process to be 43.8 kJ/mol. A physicochemical model for the alloy–water reaction is presented in the context of the observed experimental results and relevant scientific literature.

1. Introduction

Al is a desirable energy storage material owing to its high gravimetric and volumetric energy density (31.1 MJ/kg and 83.8 MJ/L, respectively) [1]. This stored chemical potential energy can be used to produce H_2 from the reaction of Al with water as indicated in Eq. (1).

$$2Al + 6H_2O \rightarrow 2Al(OH)_3 + 3H_2 \quad \Delta H^0 = -861.1KJ \tag{1}$$

However, this reaction is normally inhibited by the thin oxide layer that forms on the surfaces of Al exposed to atmosphere. In order for Al to be used effectively as an energy storage material capable of producing H_2 from water, this mechanism of self-passivation must be circumvented. Methods of disrupting this mode of passivation to enable reaction with water have been studied extensively.

Al has been observed to corrode naturally in an atmosphere containing O_2 and in solution due to the formation of pits at the metal's surface [2]. Alternative corrosion mechanisms involving hydrated surface oxides that uniformly extend into the metal have also been proposed [3]. To date, most of the experimental work conducted on producing H_2 from the reaction of Al with water has focused on a means to

* Corresponding author. Tel.: +1 630 542 0610.
** Corresponding author.
E-mail addresses: jeffrey.ziebarth@gmail.com (J.T. Ziebarth), woodall@ecn.purdue.edu (J.M. Woodall).
0360-3199/$ – see front matter
doi:10.1016/j.ijhydene.2011.01.127

accelerate this natural corrosion by crushing the Al into a fine powder, followed by circumventing the surface oxide that ordinarily protects the Al from corrosion. This can be done by intentionally modifying the structure and integrity of the surface oxide through mechanical means such as ball milling with ceramics or salts [4–7]. Mechanical action has been reported to induce a phase change in α-Al_2O_3 layers, transforming them to γ-Al_2O_3 [4,8]. This in turn allows the oxide to become hydrated, causing a H_2-producing reaction when the hydrated front extends to the Al metal by means of OH^- diffusive transport [3].

Another way in which this surface oxide can be circumvented is by dissolution in strongly acidic or strongly alkaline solutions. At low and high pH, the surface oxide on Al is driven into solution by an electrochemical potential [9]. In this manner, the entire Al metal is free to react with water and release H_2. Typically, solutions of NaOH are chosen as the corrosion enabler [10,11]. However, these solutions are extremely corrosive, making containment of the solution an issue that must be addressed in system design [11]. H_2 evolution has also been observed in Al-based batteries using alkaline electrolytes, although in this scenario it is considered a parasitic reaction and is undesirable in battery design [12].

Various metal additives such as Ga, In, Sn, Ca, Mg, Zn and Bi have also been investigated as a means of circumventing the passive oxide on Al [13–18]. Alloying or ball milling the Al with these additives has been reported to be successful in enabling Al-water reactions. In the case of low melting point metal additives, such as Ga, In and Sn, liquid phases were observed at room temperature [14]. Embrittlement of the Al by intergranular diffusion of these metal additives is cited as reason for the Al becoming chemically active in water [16], along with prevention of the Al from forming a passivating oxide layer [14]. Ga as an alloying agent has also been reported to be successful in activating Al for use in an electrochemical cell with NaOH and HCl electrolytes [19].

The motivation for this work stems from the claims made in United States patent 4,358,291 [20], where Ga-rich liquid Al–Ga alloys were patented for the purpose of splitting water to produce H_2. Early investigations into these claims resulted in the discovery that bulk quantities of solid Al–Ga alloys also exhibited this same water-reactivity [21,22]. This discovery was eventually disclosed in United States patent application 20080056986 [23]. The binary Al–Ga alloys, however, displayed limited water-reactivity at low temperatures. Heating of the binary alloys was often required to initiate reaction, indicating the need for the sample to partially liquefy before reaction could occur. In and Sn were consequently added to the binary alloys to create a Al–Ga–In–Sn quaternary alloy. These alloys displayed considerable reactivity at lower temperatures [22,24], and the invention was disclosed in United States patent application 20080063597 [25]. Early investigations into the microstructure of these alloys indicated that In and Sn had the tendency to separate out into an unidentified phase, and it was postulated as a possible reason for the observed reaction with water at low temperatures [26]. The collective body of these investigations provided direction for all future study into the Al–Ga binary and Al–Ga–In–Sn quaternary systems, as they pertain to water-reactivity, with the ultimate goal of quantifying their reaction yield characteristics and identifying their governing reaction mechanisms.

2. Experimental setup

In order to observe the physical and chemical nature of alloys in the Al–Ga–In–Sn system with water, alloys of various compositions were fabricated and tested with experiments designed to correlate their chemical behavior with their material properties. Preliminary experiments suggested that the formation of a liquid phase in the alloys was needed for their reaction with water to be observed. In an effort to verify the existence of this mechanism and identify other possible reaction mechanisms, alloy compositions were chosen to cover two-phase regions in the Al–Ga binary system. Additionally, In and Sn were selected as additives to the Al–Ga binary system as these were hypothesized to lower the temperature at which the necessary phase liquefaction would occur. The compositions used for the experiments described in this work appear in Table 1. All alloy components used for these compositions were of 99.99% purity or higher: 99.99% Al (Alfa Aesar #42328), 99.99% Ga (Recapture Metals), 99.999% In (Alfa Aesar #14720) and Sn (Atlantic Metals & Alloys).

2.1. *Fabrication and storage*

28 wt% Al-72 wt% Ga and 50 wt% Al-50 wt% Ga compositions were made in 10 g quantities by heating in a furnace at 700 °C under N_2 for 10 h. After this 10 h duration, the furnace was turned off and allowed to return to room temperature before removing the alloys. Both alloy compositions were sealed in plastic bags purged with N_2 or Ar to minimize oxidation. The bags were in turn placed in a plastic tent purged with Ar. Alloys were cleaved as necessary to obtain samples properly sized for experimentation.

The samples of the 50 wt% Al-34 wt% Ga-11 wt% In-5 wt% Sn alloy composition were made in quantities of 10 g. Alloy components were placed in a furnace at 700 °C under N_2 for a duration of 10 h. After this time had passed, the molten material was poured out and quenched on a stainless steel pan in atmosphere. The pan itself was positioned horizontally upon a mineral oil bath so as to raise the thermal mass of the quenching system. The use of water for quenching was avoided due to the water-reactive nature of the alloys being studied. After cooling in atmosphere to a safe handling temperature, the quaternary alloy samples were sealed in plastic bags purged with N_2 or Ar to minimize oxidation, which were in turn placed in a plastic tent purged with Ar.

Table 1 – Alloy compositions used for experiments (wt%).

Al	Ga	In	Sn
28.0	72.0	0.0	0.0
50.0	50.0	0.0	0.0
50.0	34.0	11.0	5.0

2.2. Analysis of Al–Ga binary alloys

Preliminary observations indicated that the reactions of Al–Ga binary alloys with water only seemed to take place when the reacting system was heated. An experiment was therefore designed to capture and measure the H_2 yield evolved from these water splitting reactions while simultaneously measuring the temperature of reaction. By observing these two measured variables on the same time scale, a plausible reaction mechanism could be postulated. H_2 yield measurements were conducted by reacting quantities of alloy measured to the nearest mg in a flask containing distilled water and routing the produced gas via Tygon tubing into an inverted eudiometer filled with water. The procedure is similar to that outlined by Zheng [27], where initial pressure, volume and temperature conditions inside the eudiometer are recorded prior to initiation of an alloy–water reaction. By observing the change in differential pressure between the gas inside the eudiometer and the outside atmosphere, and by properly accounting for the partial pressures of air and water vapor inside the eudiometer, it was possible to calculate the moles of H_2 produced in real time over the duration of a reaction experiment. This calculation was done using the ideal gas approximation: $n = PV/RT$. Reaction temperatures were controlled via a hot plate and moderated by a water bath. Pressure and temperature data was acquired electronically and stored in Excel spreadsheets for each reaction. Theoretical molar H_2 yield was calculated by stoichiometrically equating it with the molar amount of Al assumed to be in each reacting sample as shown in Eq. (2):

$$n_{H_2,\text{theoretical}} = \frac{3(\text{mass of alloy sample})(\text{wt\% Al content of alloy})}{2 \times 26.982\ \text{g/mol}} \quad (2)$$

Thus the percent H_2 yield from each reaction could be determined as follows:

$$\%\text{Yield} = \frac{n_{H_2,\text{measured}}}{n_{H_2,\text{theoretical}}} \times 100\% \quad (3)$$

2.3. Analysis of Al–Ga–In–Sn quaternary alloy

Because the Ga–In–Sn ternary eutectic has a lower melting point than pure Ga [28,29], an Al–Ga–In–Sn quaternary alloy was fabricated with an Al content comparable to the previously analyzed Al–Ga binary alloys in an effort to induce changes in the alloy's physical and chemical characteristics. The experiments that follow were designed to study the properties of this quaternary alloy in greater detail than the binary alloys in an effort to more clearly understand their structure and chemical behavior.

2.3.1. Detecting low-temperature phase transitions with DSC

Observations of this alloy with low magnification optical microscopy or even with naked eye indicate the presence of both solid and liquid phases under room temperature conditions. DSC was selected as a tool to determine the temperature at which this phase becomes liquid. A 15.4 mg sample of 50 wt % Al-34 wt% Ga-11 wt% In-5 wt% Sn alloy was analyzed 6 days after casting using a TA Instruments DSC Q100. Alodine-coated aluminum was chosen for the pan material to minimize the risk of the sample interacting with the pan surface. In order to observe melting in the sample, it was first necessary to solidify the observed liquid phase. A cooling rate of 5°C/min was selected for this purpose. After solidification in the sample was observed, the sample was heated at 5°C/min.

2.3.2. H_2 yield measurements and kinetic analysis

Preliminary measurements of H_2 yields from the reaction 50 wt% Al-34 wt% Ga-11 wt% In-5 wt% Sn alloys with water indicated that the alloys reacted reliably at all temperatures with H_2 yields greatly surpassing those of the tested Al–Ga binary alloys. As such, the quaternary alloy was well suited to a matrix study designed to measure yield as a function of time and temperature so that kinetic parameters pertaining to the alloy–water reaction could be extrapolated. A matrix of 80 trials (8 reaction temperatures, 10 trials each) was constructed to measure reaction yields using the same measurement apparatus described Section 2.2. Small pieces of alloy of variable mass were cleaved from the casted 10 g samples of 50 wt % Al-34 wt% Ga-11 wt% In-5 wt% Sn alloys for use in the trials within 5 days of casting. Though the mass of each piece was not strictly controlled, pieces were cleaved to have a mass near 80 mg so as to not produce more H_2 than the apparatus could measure. The reaction temperature of each trial was maintained to within 1 °C of the target temperature with the aid of the previously mentioned water bath. The mass of water surrounding the sample was sufficient over the duration of the reaction to resist fluctuations in reaction temperature due to heat produced by the reaction and to ambient cooling. All reaction trials were conducted within 5 days of the date upon which the alloys were cast.

For each temperature the average fraction of unreacted alloy, $X = 1 - \%\text{Yield}/100$, was fitted to a kinetic model using the rate equation $dX/dt = -k_n(T)(X - X_a)^n$, where $k_n(T)$ is the rate constant at each temperature, n is a fractional rate order assumed to be invariant with temperature and X_a is the average sample accessibility at each temperature.[1] Using an iterative approach in MATLAB to select n and evaluate the corresponding k_n value from the given yield data, a series of curves could be plotted using the rate equation.

2.3.3. Reaction yield vs sample age

H_2 yield data was also collected from a sample of 50 wt% Al-34 wt% Ga-11 wt% In-5 wt% Sn alloy at two different points in time. These points were chosen from the date at which the alloy was originally cast in order to observe if the character of the alloy's reactivity changed with time. 10 reaction trials were conducted 3 days after casting a 50 wt% Al-34 wt% Ga-11 wt% In-5 wt% Sn alloy sample, and 10 more reaction trials were conducted on the same alloy 28 days later (31 days after casting). Both sets of trials were run with a 40 °C reaction temperature using sample pieces with an average size near 80 mg.

[1] Defined as $X_a = 1 - \max(\%\text{Yield})/100$.

2.3.4. *Structure and composition*

In order to determine the structure and composition of the 50 wt% Al-34 wt% Ga-11 wt% In-5 wt% alloy, a JEOL JSM T-300 was used to observe the fracture face of a freshly cleaved alloy sample. No polishing was used in the preparation of the sample as a result of the sample being partially liquid at room temperature. No etching was used due to the reactive nature of the alloy. SEM images and EDX data were collected from the unpolished, un-etched fracture face approximately 4 days after casting.

2.3.5. *XRD analysis of reaction product*

Samples of solid precipitate were prepared by reacting a 50 wt % Al-34 wt% Ga-11 wt% In-5 wt% Sn alloy in an excess of distilled water. 8 days after the alloy was initially cast, pieces of the alloy totaling 6.175 g were incrementally added to a beaker containing 400 mL of water at 20 °C. Vigorous reaction followed with the addition of the alloy to the beaker of water, producing H_2 gas and dispersing solid precipitate throughout the water medium. A water bath was used once more to moderate the reaction temperature. The reacting system reacted a maximum temperature of 38 °C. To isolate the precipitate from the water reagent, the mixture containing the precipitate was placed into test tubes and centrifuged, drawing excess water out to the top of the mixture. Excess water could then be drained from the precipitate sample, preparing it for drying. The isolated precipitate was left to dry on a hot plate at 50 °C for 9 days. A powder XRD pattern of the dried precipitate was taken with a Bruker D8 Focus using a Cu-Kα source.

3. Results

3.1. *Results of Al–Ga binary alloys analysis*

The reactivity of the 28 wt% Al-72 wt% Ga and 50 wt% Al-50 wt % Ga alloy compositions and their dependence on temperature were tested using the reaction flask and H_2 measurement apparatus described in Section 2.2. Neither alloy displayed reactivity when first introduced into the flask of water. The temperature of the flask water was gradually increased while observing H_2 yield. Results from tests of the 28 wt% Al-72 wt% Ga and 50 wt% Al-50 wt% Ga alloy compositions are displayed in Figs. 1 and 2, respectively. In both tests, the samples are seen to begin producing a H_2 yield immediately after reaching a reaction temperature between 26 °C and 27 °C.

3.2. *Results of Al–Ga–In–Sn quaternary alloy analysis*

3.2.1. *DSC findings*

The onset of solidification was observed at −19.06 °C as shown in Fig. 3. Subsequent heating at 5°C/min showed melting began at 9.38 °C. This temperature is presumed to be the eutectic isotherm for the Al–Ga–In–Sn quaternary system because it is very close to the Ga–In–Sn ternary eutectic melting point of 10.7 °C [28], and because Al has very low solubility in liquid Ga, In and Sn [29–31], The composition of this presumed eutectic was not measured, but for the reasons previously stated is expected to contain less than 1 wt% Al.

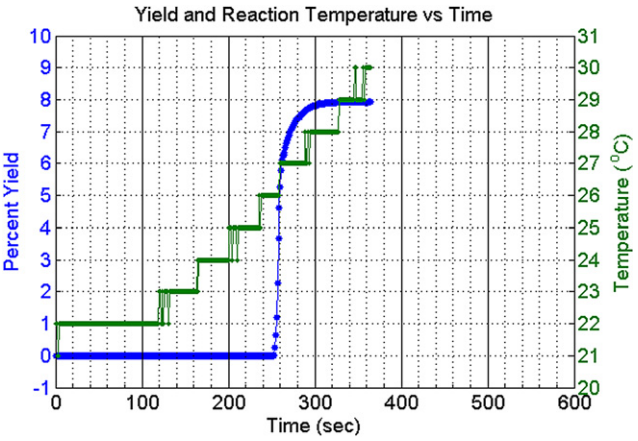

Fig. 1 – Percent yield of a 0.478 g sample of 28 wt% Al-72 wt % Ga alloy and reaction temperature versus time.

Results of the heating portion of the temperature cycle are plotted in Fig. 4. The results of both plots indicate that the observed phase is able to cool by approximately 28 °C below its melting point before solidifying.

3.2.2. *Reaction yield and kinetics*

The average yield from all 80 trials was 83.8%. Yield measurements from the matrix study are plotted in Fig. 5 for 4 of the 8 temperatures tested (alternating temperatures were omitted for the sake of graph clarity). It was determined that an n value of 0.7 could produce curves that most closely fit the measured yield data and was therefore selected as the rate order of the alloy–water reaction. The corresponding k_n for the 8 temperatures are plotted in Fig. 6. The plot gives an apparent activation energy of $E_a = 43.8$ kJ/mol.

3.2.3. *Sample age and yield*

The average percent yield from each trial set is plotted in Fig. 7 along with the sample standard deviation for each set. The sample standard deviation is shown to be much greater in the "31 day" data set. As suggested by the average yield curve for

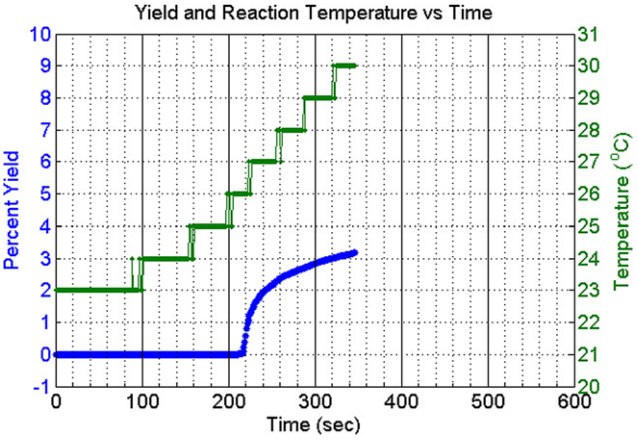

Fig. 2 – Percent yield of a 0.485 g sample of 50 wt% Al-50 wt % Ga alloy and reaction temperature versus time.

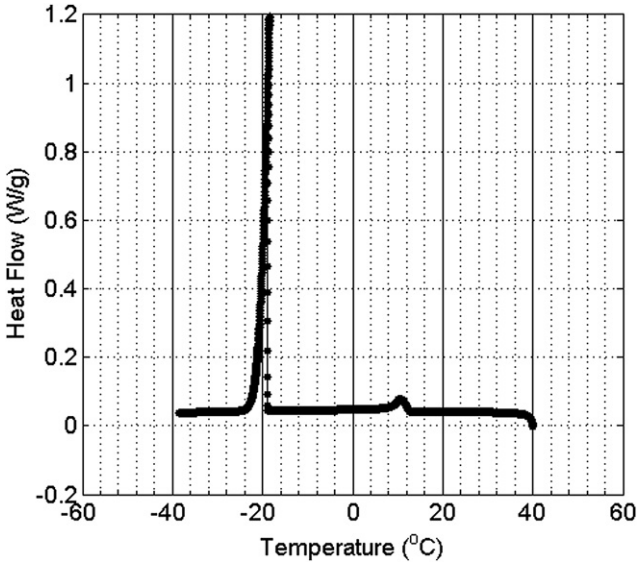

Fig. 3 – DSC cooling curve for a 15.4 mg sample of 50 wt% Al-34 wt% Ga-11 wt% In-5 wt% Sn alloy.

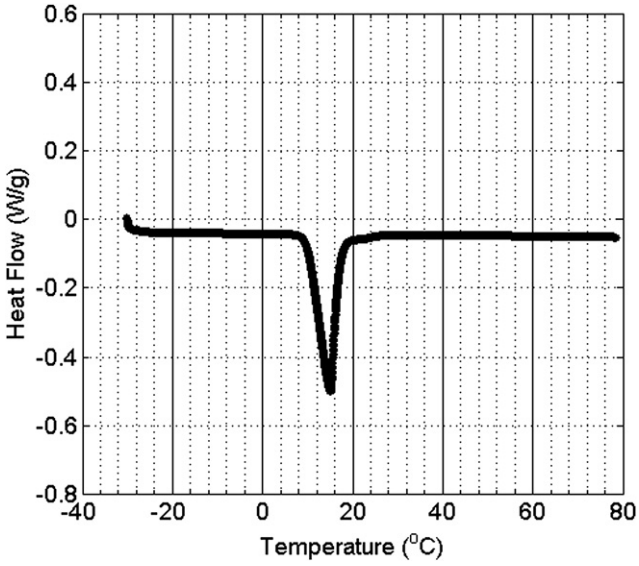

Fig. 4 – DSC heating curve for a 15.4 mg sample of 50 wt% Al-34 wt% Ga-11 wt% In-5 wt% Sn alloy.

the "31 day" data set, some trials in fact produced considerably more than the predicted 100% yield, indicating that alloy pieces in those trials had more (over 50 wt%) Al content than assumed using Eq. (2).

3.2.4. *SEM and EDX observations*

The most notable structure observed with SEM was a granular structure found near the surface of the cast wall, as pictured in Fig. 8. A thin columnar structure can also be seen at the surface. EDX data from the regions marked in Fig. 8 is listed in Table 2. EDX data shows that the granular region is primarily composed of In and Sn, with the surface columnar structure being slightly more rich in Al.

3.2.5. *Powder XRD results*

The resulting diffraction pattern is displayed in Fig. 9, with diffraction peaks corresponding to crystal planes of $Al(OH)_3$ (bayerite, JCPDS files #20-0011 and #83-2256) and In_3Sn (JCPDS file #07-0345). Given that the reaction precipitate was never heated above 50 °C, the presence of $Al(OH)_3$ is expected since it is predicted to be the stable hydroxide/oxide product below 72 °C at 1 atm of pressure [32]. The intermetallic In_3Sn found in the prepared powder is consistent with the observed In–Sn rich structure in Fig. 8.

4. Theory and discussion

A cursory review of the experiments presented here indicate that the presence of a liquid phase in the Al–Ga and Al–Ga–In–Sn alloys is necessary for the alloys to react with water and produce H_2. Both the 28 wt% Al-72 wt% Ga and 50 wt % Al-50 wt% Ga alloys display no reactivity below 26 °C as seen in Figs. 1 and 2. However as the temperature is increased, H_2 evolution indicative of reaction is observed. The onset of reaction in both alloys occurred between 26 °C and 27 °C, which correlates precisely with the reported melting point of 26.6 °C [29] for the Al–Ga binary eutectic.

The 50 wt% Al-34 wt% Ga-11 wt% In-5 wt% Sn composition produced a reaction instantaneously in water for all of the 8 tested temperatures. This is consistent with DSC measurements indicating that the liquid phase present in this alloy at room temperature solidifies well below the freezing point of water. The average percent yield and yield variance of this alloy is observed to change considerably in 4 weeks as seen in Fig. 7. This suggests a coarsening of the microstructure took place, accelerated by the fact that the alloy remained partially liquid while stored at room temperature. A redistribution of the Al content in the alloy's microstructure as a result of coarsening serves as a plausible explanation for the fact that, in some trials, alloy samples produced more H_2 than theoretically possible for a 50 wt% Al alloy. Ga, In and Sn take no part in this reaction to produce H_2 [32], the excess H_2 observed must necessarily come from an excess of Al. This is presented as further evidence in support of the claim of coarsening-influenced yields.

4.1. *Phase composition and segregation*

A solid phase of Al is expected to form first upon cooling a single phase 50 wt% Al-34 wt% Ga-11 wt% In-5 wt% Sn liquid at 700 °C to room temperature. This solid Al phase will contain some Ga and negligible amounts of In and Sn, since Ga is highly soluble in solid Al while In and Sn are not [29–31]. The presence of In_3Sn in the XRD analysis of post-reaction precipitates indicates that a second solid phase formed during casting of the alloy. As discussed previously, the liquid phase shown by DSC to be present at room temperature will have a composition similar to that of the Ga–In–Sn ternary eutectic. This liquid is expected to contain only a small weight fraction of Al. The pronounced undercooling of the eutectic in this system noted in the DSC results is hypothesized to be

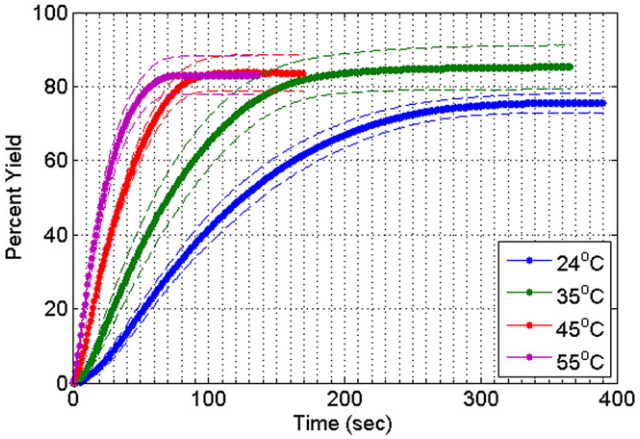

Fig. 5 – Average H_2 yield (solid lines, mean) with error bounds (dashed lines, sample standard deviation) from 50 wt% Al-34 wt% Ga-11 wt% In-5 wt% Sn alloys versus time and temperature.

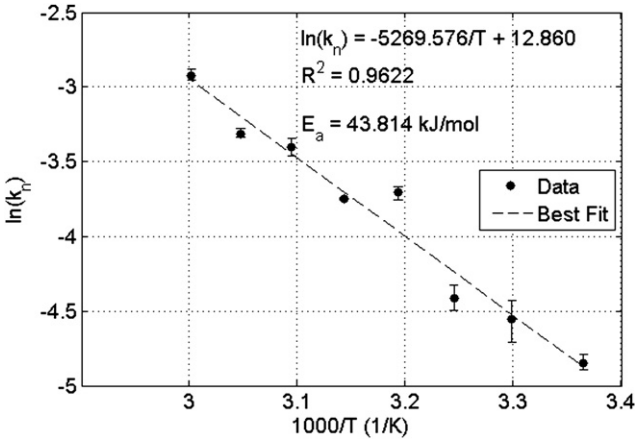

Fig. 6 – Arrhenius plot of k_n values from the reaction of a 50 wt% Al-34 wt% Ga-11 wt% In-5 wt% Sn alloy with water.

a consequence of the dissimilarities in crystal structure between the primary Al (cubic) and the eutectic Ga (orthorhombic), Sn (tetragonal) and β-In_3Sn (tetragonal) phases that precipitate out upon solidification.[2]

The EDX data in Table 2 shows the composition to be noticeably inhomogeneous. This inhomogeneity is likely the result of buoyant forces acting upon the solid Al phase during casting, caused by the large difference between its density and the surrounding liquid from which it forms. This hypothesis is consistent with phase density calculations [32] and the below-average concentrations of Al shown by EDX at the cast wall of the alloy.

4.2. *Physicochemical model for alloy–water reaction*

It is believed that the observed reaction is enabled by a liquid phase of Ga or Ga–In–Sn which contains a non-zero amounts of Al. When an alloy is completely solid, no reaction is observed to occur. This is likely the result of a coherent oxide layer on the alloy surface composed of α-Al_2O_3 and α-Ga_2O_3. α-Ga_2O_3 crystallizes in the same form as α-Al_2O_3 [33], so it is expected that a surface oxide of α-Al_2O_3 and α-Ga_2O_3 will provide the same resistance to corrosion as pure α-Al_2O_3 does for pure Al. When a phase transition occurs in the alloy, the solid phases retain their passivity while the liquid phase that emerges is not passivated. Al solvated in this liquid phase is able to diffuse freely, and causes reaction upon contacting water at the alloy surface. The resulting $Al(OH)_3$ precipitate will be swept away by H_2 bubbles nucleating at the alloy surface and escaping from the water. In order for this reaction to be sustained, solvated Al must continuously diffuse to the surface. As the reaction depletes the liquid phase below equilibrium concentrations of Al, Al and Ga in the surrounding solid grains will enter the liquid phase in an attempt to restore equilibrium. So long as solid grains remain in intimate contact with the surrounding liquid phase, they will be able to restore Al to the liquid that has been consumed by reaction with water at the alloy surface. It is in this way that liquid phases in Al–Ga and Al–Ga–In–Sn alloys enable the observed reactions: by providing a conduit through which Al can be transported to a reaction site. As the reaction continues, the alloy loses mass and the alloy–water reaction front moves inwards, eventually consuming all of the Al present in the alloy. However, experimental findings show that not all of the Al present in the tested alloy compositions is consumed by reaction. Samples of 50 wt% Al-34 wt% Ga-11 wt% In-5 wt% Sn alloy produced an average yield of 83.8%. It is believed that nucleation of H_2 bubbles during reaction cause some solid Al grains to be ejected from the samples, thereby separating them from the enabling liquid phase. The ejected grains are eventually passivated, and the Al they contain is no longer accessible for reaction with water. Samples of 28 wt% Al-72 wt % Ga and 50 wt% Al-50 wt% Ga displayed considerably lower

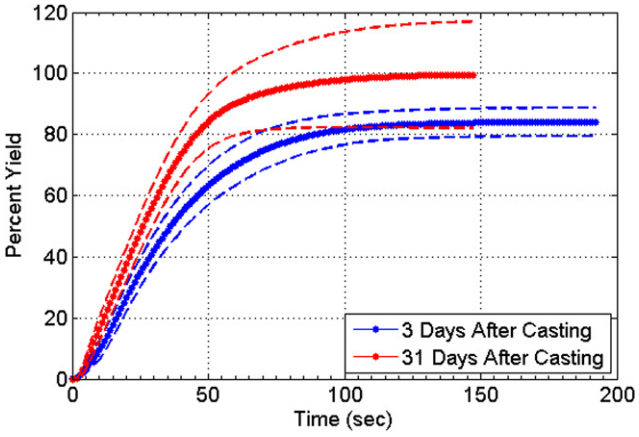

Fig. 7 – Plot showing changes in average H_2 yield (solid lines, mean) and in error bounds (dashed lines, sample standard deviation) from 50 wt% Al-34 wt% Ga-11 wt% In-5 wt% Sn alloys both 3 and 31 days after casting.

[2] The Ga–In–Sn ternary eutectic reaction is: liq. ↔ (Ga) + β + (Sn) [28].

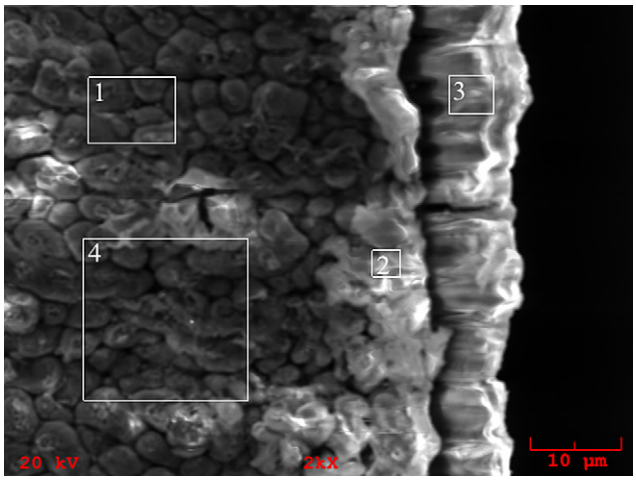

Fig. 8 – Observed microstructure at the cast wall of a 50 wt % Al-34 wt% Ga-11 wt% In-5 wt% Sn alloy sample; numbered boxes indicate regions of interest from which EDX was used to gather composition data.

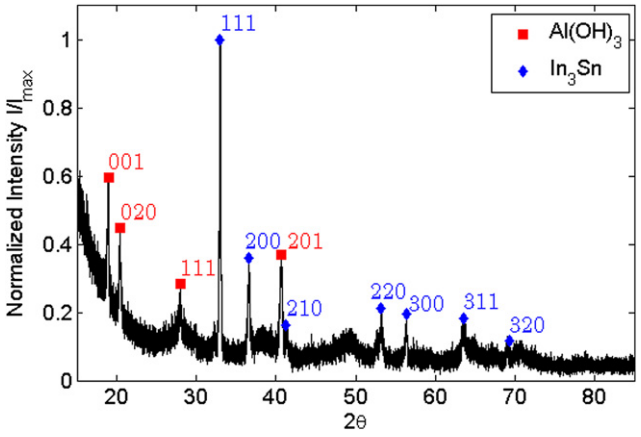

Fig. 9 – Diffraction pattern of dried powder precipitate from reaction of a 50 wt% Al-34 wt% Ga-11 wt% In-5 wt% Sn alloy with water.

yields as seen in Figs. 1 and 2. The reason for this is not fully understood, but it is postulated that the samples passivate before their eutectics can completely liquefy and that there exists in these binary alloys some microstructural barrier that restricts the free transport of solvated Al to surface reaction sites.

4.3. *Kinetics discussion*

Fractional order kinetic analysis of the collected yield data from reactions of 50 wt% Al-34 wt% Ga-11 wt% In-5 wt% Sn alloys with water indicate the alloy–water reaction has a rate order of 0.7 and an activation energy of 43.8 kJ/mol. The diffusion coefficient D_o and associated activation energy E_a for Al diffusion in liquid Ga have been experimentally determined to be 3.3×10^{-4} cm^2/s and 8.6 kJ/mol, respectively [34]. Together, the two activation energies suggest that the reaction is rate-limited by the reaction of Al with water at the alloy surface and not by the diffusive transport of Al to that surface.

The activation energy presented here is comparable to the $E_a = 42.2$ kJ/mol reported using 1st order kinetic analysis for an Al alloy–water reaction at temperatures above 125 °C [35]. However, this same paper reports a very different $E_a = 2.99$ kJ/mol for temperatures below 125 °C, suggesting different reaction mechanisms in the two temperature regimes. It is plausible that the former indicates a similar liquid phase-enabled reaction caused by phase liquefaction at temperatures above 125 °C, while the latter indicates a reaction limited by the rate at which OH^- ions can diffuse through a non-passive oxide layer created when the cited Al powders were "activated" with numerous metal additives. Further investigation, however, is needed to substantiate this hypothesis.

The rate order $n = 0.7$ reported here has also been reported in a similar study [36] where reaction rate analysis was conducted on Al–Ga–In–Sn quaternary alloys in water. However, larger activation energies were found ranging from 53 to 77 kJ/mol. The authors postulate this fluctuation is the result of variable grain size, and it may very well explain the deviation from the 43.8 kJ/mol activation energy measured in this article (though no grain sizes were measured for the 50 wt% Al-34 wt% Ga-11 wt % In-5 wt% Sn alloy samples). Furthermore, the difference in alloy compositions studied could be a potential cause for the different activation energies observed.

Table 2 – EDX data from select regions in Fig. 8.

Elt		Line	Intensity (c/s)	Error 2-sig	Conc	Units	
Region 1	Al	Kα	96.6	6.216	8.383	wt.%	
	Ga	Kα	29.87	3.456	8.188	wt.%	
	In	Lα	236	9.716	54.297	wt.%	
	Sn	Lα	114.39	6.764	28.703	wt.%	
					99.571	wt.%	Total
Region 2	Al	Kα	154.54	7.862	24.901	wt.%	
	Ga	Kα	17.23	2.625	9.678	wt.%	
	In	Lα	90.1	6.003	42.755	wt.%	
	Sn	Lα	43.87	4.189	22.666	wt.%	
					100	wt.%	Total
Region 3	Al	Kα	68.61	5.238	30.862	wt.%	
	Ga	Kα	14.75	2.429	22.217	wt.%	
	In	Lα	7.93	1.781	10.177	wt.%	
	Sn	Lα	26.12	3.232	36.332	wt.%	
					99.588	wt.%	Total
Region 4	Al	Kα	29.73	3.448	6.455	wt.%	
	Ga	Kα	22.57	3.005	14.777	wt.%	
	In	Lα	85.19	5.837	46.897	wt.%	
	Sn	Lα	52.11	4.565	31.227	wt.%	
					99.356	wt.%	Total

5. Conclusions

Experimental evidence suggests that the reaction of Al–Ga and Al–Ga–In–Sn alloys with water is reaction limited and is enabled by a liquid phase through which Al can diffuse.

Reactions of Al–Ga alloys with water are enabled by liquefaction of the eutectic. DSC analysis of Al–Ga–In–Sn alloys indicates that solidification of all phases requires significant cooling such that under ambient conditions, a liquid phase exists to enable reaction with water. However, the constant presence of this liquid phase is also believed to be responsible for accelerating a coarsening effect which increases the variability in the reaction yield of older samples. Kinetic analysis of the quaternary alloy reaction has been shown to be of a fractional order 0.7 with an activation energy of 43.8 kJ/mol. The production of bayerite was confirmed by powder XRD analysis of the products from these quaternary alloy reactions. The presence of In_3Sn intermetallic in the alloy was also confirmed using XRD, and is consistent with the SEM/EDX observation of an In–Sn rich grain structure at the cast wall of the alloy.

Acknowledgments

Special thanks to Professor Elias Franses, Professor Carol Handwerker and John Koppes for their advice and assistance throughout the course of this research.

REFERENCES

[1] Lide DR, editor. CRC Handbook of chemistry and physics. 88th ed. CRC Press/Taylor and Francis; 2007.
[2] Szklarska-Smialowska Z. Pitting corrosion of aluminum. Corrosion Science 1999;41:1743–67.
[3] Bunker BC, Nelson GC, Zavadil KR, Barbour JC, Wall FD, Sullivan JP, et al. Hydration of passive oxide films on aluminum. The Journal of Physical Chemistry B 2002;106(18): 4705–13.
[4] Deng ZY, Liu YF, Tanaka Y, Ye J, Sakka Y. Modification of Al particle surfaces by γ-Al_2O_3 and its effect on the corrosion behavior of Al. Journal of the American Ceramic Society 2005; 88(4):977–9.
[5] Deng ZY, Tang YB, Zhu LL, Sakka Y, Ye J. Effect of different modification agents on hydrogen-generation by the reaction of Al with water. International Journal of Hydrogen Energy 2010;35(18):9561–8.
[6] Mahmoodi K, Alinejad B. Enhancement of hydrogen generation rate in reaction of aluminum with water. International Journal of Hydrogen Energy 2010;35(11):5227–32.
[7] Alinejad B, Mahmoodi K. A novel method for generating hydrogen by hydrolysis of highly activated aluminum nanoparticles in pure water. International Journal of Hydrogen Energy 2009;34(19):7934–8.
[8] Gates RS, Hsu M, Klaus EE. Tribochemical mechanism of alumina with water. Tribology Transactions 1989;32(3): 357–63.
[9] Pourbaix M. Atlas of electrochemical equilibria in aqueous solutions. Pergamon Press; 1966.
[10] Deng ZY, Ferreira JMF, Sakka Y. Hydrogen-generation materials for portable applications. Journal of the American Ceramic Society 2008;91(12):3825–34.
[11] Wang H, Leung D, Leung M, Ni M. A review on hydrogen production using aluminum and aluminum alloys. Renewable and Sustainable Energy Reviews 2009;13(4): 845–53.
[12] Li Q, Bjerrum NJ. Aluminum as anode for energy storage and conversion: a review. Journal of Power Sources 2002;110(1): 1–10.
[13] Parmuzina A, Kravchenko O. Activation of aluminium metal to evolve hydrogen from water. International Journal of Hydrogen Energy 2008;33(12):3073–6.
[14] Kravchenko O, Semenenko K, Bulychev B, Kalmykov K. Activation of aluminum metal and its reaction with water. Journal of Alloys and Compounds 2005;397(1–2):58–62.
[15] Fan MQ, Xu F, Sun LX. Studies on hydrogen generation characteristics of hydrolysis of the ball milling Al-based materials in pure water. International Journal of Hydrogen Energy 2007;32(14):2809–15.
[16] Trenikhin MV, Bubnov AV, Nizovskii AI, Duplyakin VK. Chemical interaction of the In-Ga eutectic with Al and Al-base alloys. Inorganic Materials 2006;42(3):256–60.
[17] Plakhotnikova NA, Gopienko VG, Kolpachev AA, Reznikova GA. Chemical reaction of aluminum alloy powders with water. Powder Metallurgy and Metal Ceramics 1988;27(8):605–8.
[18] Ilyukhina AV, Kravchenko OV, Bulychev BM, Shkolnikov EI. Mechanochemical activation of aluminum with gallams for hydrogen evolution from water. International Journal of Hydrogen Energy 2010;35(5):1905–10.
[19] Tuck CDS, Hunter JA, Scamans GM. The electrochemical behavior of Al–Ga alloys in alkaline and neutral electrolytes. Journal of the Electrochemical Society 1987;134 (12):2970–81.
[20] Cuomo JJ, Woodall JM. Solid state renewable energy supply. United States Patent 4,358,291, Nov 7 1982.
[21] Woodall JM, Ziebarth J, Allen CR. The Science and Technology of Al-Ga Alloys as a material for energy storage, transport, and splitting water. In: Proceedings of the ASME 2nd energy nanotechnology international conference, Sept 5–7, 2007, Santa Clara, CA.
[22] Woodall JM, Ziebarth JT, Allen CR, Sherman DM, Jeon J, Choi G. Recent results on splitting water with aluminum alloys. Proceedings of materials innovations in an emerging hydrogen economy, Feb 24–27, 2008, Cocoa Beach, FL.
[23] Woodall JM, Ziebarth JT, Allen CR, Jeon JH, Zheng Y, Gobel GH, Koehler KC, Salzman DB, Harmon ES. Power generation from solid aluminum. United States Patent Application 20080056986, Filed May 11, 2007.
[24] Woodall JM, Ziebarth JT, Allen CR, Jeon J, Choi G, Kramer R. Generating hydrogen on demand by splitting water with Al rich alloys. Proceedings of the 2008 clean technology conference and trade show, June 1–5, 2008, Boston, MA.
[25] Woodall JM, Ziebarth JT, Allen CR. Power generation from solid aluminum. United States Patent Application 20080063597, Filed Sept 5, 2007.
[26] Ziebarth JT, Woodall J, Choi G, Allen CR, Jeon JH, Sherman D, Kramer R. Splitting Water with Al Rich Alloys: Structure and Reaction Kinetics. TMS 2009 Annual Meeting and Exhibition, February 15–19, 2009, San Francisco, CA.
[27] Zheng F, Rassat SD, Helderandt DJ, Caldwell DD, Aardahl CL, Autrey T, et al. Automated gas burette system for evolved hydrogen measurements. Review of Scientific Instruments 2008;79(8):084103.
[28] Evans DS, Prince A. Thermal analysis of Ga–In–Sn system. Metal Science 1978;12(9):411–4.
[29] Murray JL. The Al–Ga (aluminum–gallium) system. Journal of Phase Equilibria 1983;4(2):183–90.
[30] Murray JL. The Al–In (aluminum–indium) system. Journal of Phase Equilibria 1983;4(3):271–8.
[31] McAlister AJ, Kahan DJ. The Al–Sn (aluminum–tin) system. Journal of Phase Equilibria 1983;4(4):410–4.
[32] Ziebarth JT. Use of the Al–Ga–In–Sn system for energy storage and conversion, Purdue University; 2010, PhD thesis.

[33] Zinkevich M, Aldinger F. Thermodynamic assessment of the gallium-oxygen system. Journal of the American Ceramic Society 2004;87(4):683–91.
[34] Bräuer P, Müller-Vogt G. Measurements of aluminum diffusion in molten gallium and indium. Journal of Crystal Growth 1998;186(4):520–7.
[35] Zasukha VA, Kozin LF, Danil'tsev BI. Kinetics of the reduction of water by activated aluminum powder. Theoretical and Experimental Chemistry 1995;31(4):196–9.
[36] Wang W, Chen DM, Yang K. Investigation on microstructure and hydrogen generation performance of Al-rich alloys. International Journal of Hydrogen Energy 2010;35(21):12011–9.